

The diffuse neutrino flux from FR-II radio galaxies and blazars: A source property based estimate

Julia K. Becker ^{a,*}, Peter L. Biermann ^{b,c}, Wolfgang Rhode ^a

^a*Department of Physics, Dortmund University, D-44221 Dortmund, Germany*

^b*Max Planck Institut für Radioastronomie, Auf dem Hügel 69, D-53121 Bonn, Germany*

^c*Department of Physics and Astronomy, University of Bonn, Germany*

Abstract

Water and ice Cherenkov telescopes of the present and future aim for the detection of a neutrino signal from extraterrestrial sources at energies $E_\nu > \text{PeV}$ [Woschnagg and AMANDA Collaboration (2004); Montaruli (2003); IceCube Collaboration (2004)]. Some of the most promising extragalactic sources are Active Galactic Nuclei (AGN). In this paper, the neutrino flux from two kinds of AGN sources will be estimated assuming $p\gamma$ interactions in the jets of the AGN. The first analyzed sample contains FR-II radio galaxies while the second AGN type examined are blazars. The result is highly dependent on the proton's index of the energy spectrum. To normalize the spectrum, the connection between neutrino and disk luminosity will be used by applying the jet-disk symbiosis model from Falcke and Biermann (1995). The maximum proton energy and thus, also the maximum neutrino energy of the source is connected to its disk luminosity, which was shown by Lovelace (1976) and was confirmed by Falcke et al. (1995).

Key words: Neutrinos, FR-II, blazars, jet-disk symbiosis, AMANDA, IceCube

PACS: 95.55.Vj, 98.54.-h, 98.62.-g, 98.70.Sa

1 Introduction

Large volume neutrino telescopes like AMANDA, Antares and IceCube [Woschnagg and AMANDA Col (2004); Montaruli (2003); IceCube Collaboration (2004)] are being built to detect the neutrino flux from extraterrestrial sources. For a diffuse analysis, the

* Corresponding author. Contact: julia@physik.uni-dortmund.de, phone: +49-231-7553667

detection of such a signal is possible at energies at which the extragalactic neutrino flux contribution exceeds the number of atmospheric neutrinos. Active Galactic Nuclei (AGN) are believed to make up a large fraction of the extragalactic neutrino flux. While previous models - see e.g. [Learned and Mannheim (2000)] for a review - used the Cosmic Ray flux or a certain part of the photon spectrum to estimate the neutrino flux from AGN, the model presented in this paper uses the jet-disk symbiosis model by Falcke and Biermann (1995) and allows for the dependence of the maximum particle energy on the source properties. This is the key point of our analysis.

The total neutrino spectrum at Earth is given as

$$\Phi(E_\nu^0) = \int_z \int_L dz dL \frac{dN}{dE_\nu}(E_\nu^0, L, z) \cdot \frac{dn}{dL}(L, z) \cdot \frac{dV}{dz} \cdot \frac{1}{4\pi d_L(z)^2}. \quad (1)$$

The parameters in the calculation are the integral radio luminosity L and the redshift z . The energy of the neutrinos at the source E_ν is redshifted due to adiabatic energy losses on the particles' way toward Earth, $E_\nu = (1+z) \cdot E_\nu^0$, where E_ν^0 is the neutrinos' energy at Earth. dN/dE_ν is the single source spectrum of an AGN, while dn/dL is the radio luminosity function (RLF) per comoving volume dV/dz and luminosity interval. To obtain the total number of AGN per redshift interval, the RLF has to be weighted by the comoving volume and divided by a factor of $4\pi d_L^2$ with d_L as the luminosity distance to receive the neutrino flux at Earth. Finally, the result has to be integrated over all possible redshifts and luminosities, where the integration limits depend on the source sample as discussed in section 4.

The neutrino flux will be calculated for two different source samples, one including FR-II sources with strong extended radio emission (in the following referred to as "steep spectrum sources") and the second one flat spectrum blazar sources (referred to as "flat spectrum sources" throughout the paper). It will be assumed that neutrinos are produced by pions resulting from a Δ -resonance of the initial $p\gamma$ interaction. In this scenario, the neutrino spectrum follows the proton spectrum. Multipion events (see e.g. [Mücke et al. (1999)]) will not be included in this calculation, since the changes of the spectrum due to these events would lie within the estimated uncertainty of the calculation due to uncertainties in the jet-disk symbiosis model and the sources' Radio Luminosity Functions (RLFs), see section 5.2. For the steep spectrum sources, the spectral index of the proton spectrum will be calculated from the synchrotron emission of the electrons. This is possible since the proton and electron spectra resulting from shock acceleration are equivalent. This method cannot be used for the flat spectrum source sample, since the radio emission of the jet is spatially unresolved and therefore, the observed spectrum is a superposition of the different radio spectra. In this case, the spectrum will be a superposition of the spectra of all knots, each with a particle index of

$p \simeq 2$, following the derivation of the index in diffuse shock acceleration, see e.g. [Protheroe (1998)]. The maximum energy of the protons in the jets will be assumed to be luminosity dependent as is suggested in [Lovell (1976)]. To normalize the generic AGN energy spectrum, the jet-disk symbiosis model given in [Falcke et al. (1995)] will be applied to connect the neutrino luminosity with the disk luminosity and therefore, also with the radio luminosity of the jets. Throughout this paper, an Einstein-de Sitter Universe ($\Omega_m = 1$, $\Omega_\Lambda = 0$) with $h = 0.5$ is assumed, since the used RLFs are not available in the concordance model ($\Omega_m \approx 0.3$, $\Omega_\Lambda \approx 0.7$) which has been confirmed by recent measurements [Spergel et al. (2003)]. However, the result should be independent of the cosmology used as it has been pointed out in [Dunlop and Peacock (1990)].

The paper is organized as follows: In section 2, the two AGN samples will be discussed. They will be used to determine the AGN radio luminosity function (RLF). In case of the steep spectrum sources, the spectral indices between 2.7 and 5 GHz are used to evaluate the index of the primary particle spectrum. Section 3 gives an explicit description of the normalization of the single source spectrum to the disk luminosity of the objects. In section 4, the integration limits for the redshift and luminosity distribution are discussed. Finally, the different models for both types of AGN sources are applied to calculate the AGN neutrino flux. It will be shown that the result strongly depends on the index of the particle spectrum.

2 The samples

The first sample consists of 356 steep spectrum sources, selected by Willott et al. (2001). The sources are sampled from the 7CRS [McGilchrist and Riley (1990); Lacy et al. (1999)], 6CE [Rawlings et al. (2001)] and 3CRR [Laing et al. (1983)] catalogs with flux measurements at 178 MHz. The second sample comprises 171 flat spectrum sources from Dunlop and Peacock (1990). They are selected from the Parkes selected regions sample, the Parkes $\pm 4^\circ$ zone [Peacock (1985); Wright et al. (1982)], the 'Northern-Sky' survey of Peacock and Wall (1981) and the 'All-Sky' survey of Wall and Peacock (1985).

2.1 *The spectral and particle index of the sources*

As discussed in detail in, e.g., [Rybicki and Lightman (1979)], the index p of the proton spectrum is correlated to the index α of synchrotron radiation by $p = 2\alpha + 1$.

2.1.1 Steep spectrum sources

123 of the total 356 sources are identified in the S1-S5 catalogs [Pauliny-Toth et al. (1972); Pauliny-Toth and Kellermann (1972); Pauliny-Toth et al. (1978); Kühr et al. (1981)] which give the spectral index of the sources at 2.7–5 GHz. To estimate the steep spectrum index α_s at 2.7–5 GHz, the maximum in a distribution of the source counts versus α_s is determined applying a Gauß fit (see Fig. 1). The maximum is found to be at $\alpha_s = 0.8$ with a peak width of $\sigma_s = 0.2$. In calculations of the AGN evolution functions by Willott et al., a spectral index of $\alpha_s = 0.8$ is assumed [Willott et al. (2001)]. The spot check of the sources supports this assumption. Hence, the index of $\alpha = 0.8$ is adopted. This result is supported by Gregorini et al. (1984) who analyze the spectral index of radio galaxies in the range of 2.7 to 5 GHz resulting in an average index of around 0.8 for steep spectra. Consequently the particle index is $p_s = 2 \cdot \alpha_s + 1 = 2.6$. Here, it is assumed that the stationary particle spectrum is equal to the particle injection spectrum, which is based on the assumption that particles from this region undergo energy scale independent losses such as would occur in a flow. There is unfortunately no good and well-tested model available at this time for the particle transport, convection versus diffusion and other processes, so that we make this simple assumption by Occam’s razor. To demonstrate the influence of the particle index on the resulting spectrum, the calculation will also be done with different harder spectral indices.

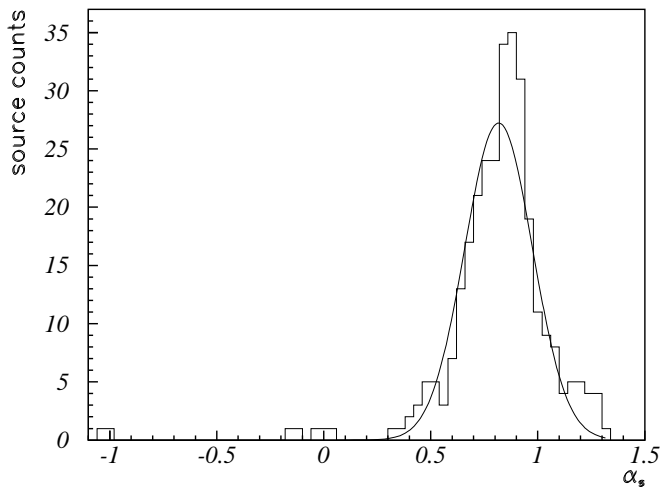


Fig. 1. Histogram of the spectral indices of the steep spectrum sources. Source counts are shown against the spectral index at 5 GHz. The maximum is found at $\alpha_s = 0.8$. The width of the Gauß distribution is $\sigma_s = 0.2$.

2.1.2 Flat spectrum sources

Since the radio spectrum of blazars is spatially unresolved, the observed index of the radio spectrum cannot be identified with the index of synchrotron radiation. The particle spectrum is a superposition of the spectra of the single knots,

$$dN/dE_\nu \propto \sum_i a_i E^{-p}$$

assuming the same particle index for all sources, $p \simeq 2$, as suggested by diffuse shock acceleration for strong shocks, and also by the radio data of strong jets. An index close to $p \simeq 2$ is supported by the individual radio spectra as described in, e.g., [Bridle and Perley (1984)] for strong sources.

2.2 Radio Luminosity Functions

2.2.1 Steep spectrum sources

The AGN RLF depends on the luminosity and on the redshift. To find the proper relation empirically, a factorizing separation of the density in a luminosity dependent function and a redshift dependent distribution is assumed by Willott et al. (2001). The model includes the steep spectrum sources as they are explained above. The AGN RLF is given at a frequency of 0.151 GHz depending on the differential luminosity $L_{0.151}$. The RLF was assumed to consist of two separate distributions, a low luminosity function including objects without or with only weak emission lines and a high luminosity function with objects with strong emission lines. The density $\rho(L_{0.151}, z)$ is given as the product of a pure luminosity function $\rho_l(L_{0.151})$ in units of $1/(\text{Gpc}^3 \Delta \log L_{0.151})$ and the dimensionless evolution function $f(z)$:

$$\rho(L_{0.151}, z) = \rho(L_{0.151}) \cdot f(z).$$

Two AGN populations contribute to the RLF:

Low luminosity sources only show weak or no emission lines. These sources are FR-I and weak emission line FR-II galaxies. Above a luminosity $L_{0.151} \approx 10^{25.5} \text{ W}/(\text{Hz sr})$, the sources can almost exclusively be assumed to be FR-II galaxies. For the low luminosity function, $\rho_l(L)$, an ansatz of

$$\rho_l(L_{0.151}) = \rho_l^0 \left(\frac{L_{0.151}}{L_l^*} \right)^{-\alpha_l} \cdot \exp \left[-\frac{L_{0.151}}{L_l^*} \right]$$

is made. This analytic ansatz is known as the Schechter function in literature [Schechter (1976)]. α_l is the power law shape, ρ_l^0 is the normalization constant and L_l^* is the break luminosity. The evolution function of the low luminosity population is taken to be

$$f_l(z) = \begin{cases} (1+z)^{\alpha_l} & \text{for } z \leq z_l^0 \\ (1+z_l^0)^{\alpha_l} & \text{for } z > z_l^0. \end{cases}$$

The redshift evolution of the sources is known up to $\sim z_l^0$. At higher redshifts, it is assumed to be constant since there are experimental indications [Miyaji et al. (2000)] of a constant or slightly decreasing distribution at redshifts up to $z \sim 6$. The values of five free parameters used in the functions are listed in table 1. The complete (luminosity and redshift dependent) RLF is shown in Fig. 2.

The high luminosity population consists of FR-II galaxies with strong emission lines. The form of the high luminosity function, $\rho_h(L_{0.151})$, is similar to the one for the low luminosity population. Here, however, the exponential function applies at low luminosities while the power law dominates at higher luminosities:

$$\rho_h(L_{0.151}) = \rho_h^0 \left(\frac{L_{0.151}}{L_h^*} \right)^{-\alpha_h} \cdot \exp \left[-\frac{L_h^*}{L_{0.151}} \right].$$

The evolution function of the high luminosity population is assumed to be an exponential function up to a certain redshift z_h^0 and then continuing as a constant:

$$f_h(z) = \begin{cases} \exp \left[-\frac{1}{2} \left(\frac{z-z_h^0}{z_h^0} \right)^2 \right] & \text{for } z \leq z_h^0 \\ 1 & \text{for } z > z_h^0. \end{cases}$$

A comparison to X-ray data [Miyaji et al. (2000)] justifies an exponentially increasing evolution.

The luminosity, which is here given at 0.151 GHz, is used in the integral form for further calculations. Thus the luminosity $L_{0.151}$ is converted to the integral radio luminosity in units of 10^{42} erg/s, L_{42} , by assuming a spectral index of $\alpha = 0.8$. Furthermore, the RLF is given in units of $\text{Gpc}^{-3} (\Delta \log(L))^{-1}$. In following calculations, the RLF will be given per luminosity interval dL_{42} .

ρ_l^0	α_l	L_l^*	z_l^0	k_l	ρ_h^0	α_h	L_h^*	z_h^0	z_h^1
$10^{1.850}$	0.542	$10^{26.14}$	0.646	4.10	$10^{-6.260}$	2.31	$10^{26.98}$	1.81	0.523

Table 1

Parameters used in the calculation of the AGN RLF for steep spectrum sources [Willott et al. (2001)]. ρ_l^0 and ρ_h^0 are given in units $\text{Gpc}^{-3}\Delta(\log L)$. L_h^* and L_l^* are given in $\text{W}/(\text{Hz sr})$.

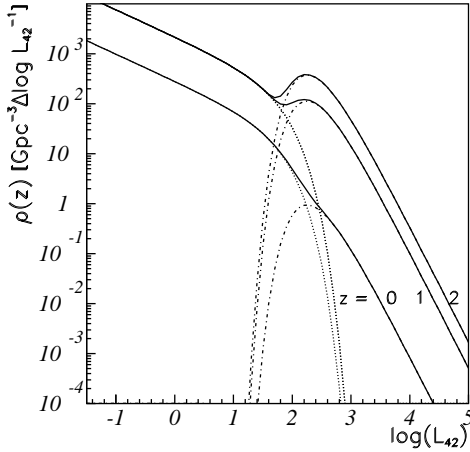


Fig. 2. Steep spectrum RLF according to Willott et al. (2001) versus luminosity for $z = 0, 1, 2$.

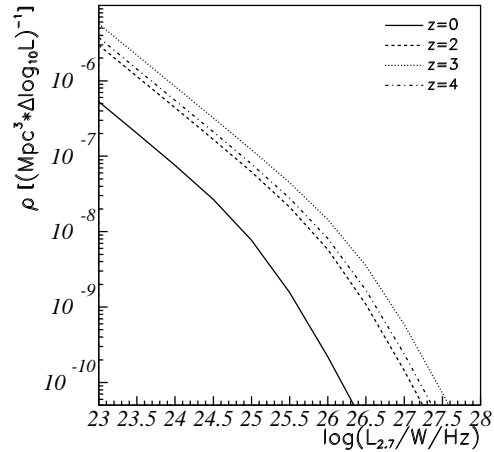


Fig. 3. RLF for flat spectrum sources in a pure luminosity evolution model according to Dunlop and Peacock (1990). Four different redshift values are used, $z = 0, 2, 3, 4$.

2.2.2 Flat spectrum sources

171 flat sources from four catalogs at 2.7 GHz are used by Dunlop and Peacock (1990) to determine the RLF of flat spectrum blazars as described above. The ansatz for the flat spectrum RLF is a pure luminosity evolution function of the form

$$\rho(L, z) = \rho_0 \cdot \left\{ \left(\frac{L}{L_c(z)} \right)^\alpha + \left(\frac{L}{L_c(z)} \right)^\beta \right\}^{-1}.$$

The function is labeled pure luminosity evolution since only the break luminosity L_c evolves with the redshift. Here, α and β are the power law slopes, ρ_0 is the normalization and $L_c(z)$ is the break luminosity which evolves with redshift:

$$\log[L_c(z)] = a_0 + a_1 \cdot z + a_2 \cdot z^2.$$

The luminosity L is given in units of W/(Hz sr) at a frequency of 2.7 GHz. The RLF is shown in Fig. 3 with the set of parameters as given in table 2. For further calculations, the luminosity at 2.7 GHz is converted to an integral luminosity by assuming a flat spectrum with $\alpha_f = 0$. The RLF is given in units of $\text{Gpc}^{-3} \cdot (\Delta \log L)^{-1}$, and thus the differential RLF is

$$\frac{dn}{dL}(L, z) = \frac{\rho_0}{\ln(10) \cdot L} \cdot \left\{ \left(\frac{L}{L_c(z)} \right)^\alpha + \left(\frac{L}{L_c(z)} \right)^\beta \right\}^{-1}. \quad (2)$$

ρ_0	α	β	a_0	a_1	a_2
$10^{0.85} \text{ Gpc}^{-3}$	0.83	1.96	24.89	1.18	-0.28

Table 2
Parameters for the flat spectrum RLF [Peacock (1985)].

3 The single source spectrum

The generic AGN neutrino flux is adopted to follow the proton spectrum from the Δ -decay. This can be described as a power law with an index p having an exponential cutoff. This cutoff depends on the particle's maximum energy. Also, the power of the spectrum changes by -2 when synchrotron losses of pions start to dominate at energies of $E_\nu^{break} \approx E_\nu^{\max}/6.7$. The break energy is determined by the ratio of the pion's to the protons mass, $m_\pi/m_p = 1/6.7$, since the maximum energy due to synchrotron losses of a charged particle is proportional to the particles mass [Biermann and Strittmatter (1987)]. The spectrum is then given as

$$\frac{dN}{dE_\nu} = \begin{cases} \phi_\nu(L_{disk}) \cdot E_\nu^{-p} \exp\left(-\frac{E_\nu}{E_\nu^{\max}}\right) & \text{for } E_\nu < E_\nu^{break} \\ \phi_\nu(L_{disk}) \cdot E_\nu^{-p} \left(E_\nu/E_\nu^{break}\right)^{-2} \exp\left(-\frac{E_\nu}{E_\nu^{\max}}\right) & \text{for } E_\nu \geq E_\nu^{break} \end{cases}. \quad (3)$$

The power law behavior is due to diffuse shock acceleration of the protons in the jet's shock fronts. The spectrum is limited by the strength of the magnetic field of the source due to the spatial limit of the Larmor motion [Hillas (1984)]. This determines the maximum energy of the accelerated protons, there is an exponential cutoff in the spectrum. The magnetic field is connected to the disk luminosity of the AGN and subsequently the maximum proton energy can be expressed in terms of the disk luminosity, see [Lovelace (1976)]:

$$E_p^{\max} \propto \sqrt{L_{disk}}$$

as it has been confirmed by the jet-disk symbiosis model, see [Falcke and Biermann (1995)]. At high luminosities of $L_{disk} > 10^{46}$ erg/s Biermann (2001), a saturation of the proton maximum energy is expected due to photo-pion production in the disk radiation field. This effect will be discussed in section 4.

The normalization of the generic neutrino spectrum, ϕ_0 , can be found by assuming that particles from an AGN produce the same order of magnitude of luminosity as the jet power, Q_{jet} , and neutrinos contribute with a fraction $q_\nu < 1$ [Falcke et al. (1995)]. The observations are best fitted by this concept and this number constraint. It is assumed that the power of the neutrinos is directly connected to the power of the jet. This in turn is a fraction $q \geq 1/3$ of the disk luminosity. Here we use the lower limit, $q = 1/3$, as an estimate. The factor q_ν results from assuming a kinematic factor of $\xi_{kin} \approx 1/2$ which accounts for the fact that only half of the protons are converted into pions - about 50% of the protons convert into neutrons [Mücke et al. (2000)]. Additionally, a (non thermal) efficiency of $\epsilon_{nth} \approx 10\%$ is applied - 20% of the proton energy goes into secondary mesons and 50% of these 20% go into neutrino production. The optical depth of AGN sources $\tau_{p\gamma}$ can be described as the product of the photohadronic cross section $\sigma_{p\gamma}$ and the photon density n_γ , and thus

$$\tau_{p\gamma} \approx 800 \frac{L_{46}}{r_{17}}.$$

Here, $r_{17} := r/10^{17}$ cm is the extension of the source in units of 10^{17} cm. Scaling this optical depth to the Eddington luminosity and to the Schwarzschild radius demonstrates that the optical depth is independent of the power of the source at equivalent distances from the central engine. It also shows that large optical depths are easily achieved. The neutrino measurements can then be used to set limits on the optical depths, and so on the structure of the emitting region, as we show below. Taking into account interactions of protons in Bethe-Heitler pair production, an effective opacity for photopion production is reduced to

$$\tau_{eff} = \tau_{p\gamma} \cdot \eta.$$

η gives the reduction of the optical depth due to the optical depth of the source taking into account Bethe Heitler interactions, τ_{BH} . In all following calculations, $\tau_{eff} = 1$ will be assumed. Detailed geometric models for emission from zones where the effective optical depth is large, where it is close to unity, and where it is much less than unity, need to be considered in a later stage of such calculations. This might be easier in the future once there are good constraints, or even exact spectra from multi-GeV to multi-TeV observations of AGN. Since the neutrino flux is proportional to τ_{eff} , a lower limit as an estimate of a maximal optical depth is possible when comparing current neutrino flux limits to the calculated flux as it is described in section 5.4.

The fraction q_ν is then

$$q_\nu = q \cdot \tau_{eff} \cdot \xi_{kin} \cdot \epsilon_{nth} \approx \frac{1}{60}.$$

Thus the neutrino luminosity from the jets is given as a fraction of the disk luminosity:

$$\begin{aligned} \int_{E_\nu^{\min}}^{E_\nu^{\max}} E_\nu \cdot \frac{dN}{dE_\nu} \cdot dE_\nu &= \int_{E_\nu^{\min}}^{E_\nu^{break}} \phi_\nu \cdot E_\nu^{-p+1} \exp\left(-\frac{E_\nu}{E_\nu^{\max}}\right) dE_\nu \\ &+ \int_{E_\nu^{break}}^{E_\nu^{\max}} \phi_\nu \cdot E_\nu^{-p-1} \cdot E_\nu^{break^2} \exp\left(-\frac{E_\nu}{E_\nu^{\max}}\right) dE_\nu = q_\nu \cdot L_{disk}. \end{aligned}$$

The integral can be evaluated by developing the exponential function in a Taylor series and interchanging the integral with the sum. The lower integration limit is a fraction of 1/4 of the rest mass of the pion, $E_\nu^{\min} = E_{\pi^\pm}^0/4 = (139.57018 \pm 0.00035)/4$ MeV, [Particle Data Group (2004)]. The upper integration limit is assumed to be varying with the disk luminosity, see Equ. (8).

The normalization is thus given as

$$\begin{aligned} x L_{disk} &= \ln\left(\frac{E_\nu^{\max}}{E_\nu^{\min}}\right) + \{f(p-2, 1/6.7, 0) \\ &+ [f(p, 1, 0) - f(p, 6.7, 0)]/6.7^2\} \cdot E_\nu^{\max-p+2} \\ &- f(p-2, E_\nu^{\max}/E_\nu^{\min}, -p+2) \cdot E_\nu^{\min-p+2} \end{aligned}$$

with

$$f(a, b, c) = \sum_{n=0, n \neq a}^{\infty} \frac{(-1)^n}{n! \cdot (n-a)} b^{-n+a+c}.$$

The series' are evaluated numerically for each case.

3.1 Jet-disk symbiosis

To convert the disk luminosity into the radio luminosity of the jets, the jet-disk symbiosis model by Falcke et al. (1995) is used.

3.1.1 Flat spectrum sources

Assuming a power law slope of $\alpha = 0$ the luminosity of the jet in units of erg/s, L^f is given as [Falcke and Biermann (1995)]

$$L^f = 6.7 \cdot 10^{42} \frac{\text{erg}}{\text{s}} \cdot D^{2.17} \cdot \sin^{0.17}(i_{\text{obs}}) \cdot (x'_e)^{0.83} \cdot \left(\frac{6}{\gamma_j}\right)^{1.8} \cdot q_{j/1}^{1.42} \cdot L_{46}^{1.42-\xi}. \quad (4)$$

Parameters appearing in Equ. 4 are given in the parameter list below. In using here $\alpha = 0$ instead of the sum of components with $\alpha = 1/2$ we follow the earlier work. It is not known what the energetic particle spectrum does at low energies in the jet. For the final conclusion below we do use $p = 2$, which would correspond to $\alpha = 1/2$ if pure synchrotron radiation was observed.

The parameters from above are defined in the parameter list below. The correlation between disk luminosity and radio luminosity in units of 10^{42} erg/s, L_{42}^f , is

$$L_{\text{disk}} = (2.1 \pm 1.9) \cdot 10^{45} (L_{42}^f)^{0.79} \left[\frac{\text{erg}}{\text{s}} \right]. \quad (5)$$

The error has been estimated by taking into account a scattering of the data by about a factor three around $L_{42}^f(L_{\text{disk}})$.

3.1.2 Steep spectrum sources

The model for extended, optically thin sources will additionally be used for the calculation of the steep spectrum source flux. The relation between the differential radio luminosity at 5 GHz of the lobes and the disk luminosity is

$$P_{\text{lobe}} = 1.8 \cdot 10^{34} \frac{\text{erg}}{\text{s} \cdot \text{Hz}} \left(\frac{\text{GHz}}{\nu} \right)^{0.5} \cdot \frac{\beta_j^{1/4} \cdot P_{-12}^{1/4} \cdot x'_{e,100} \cdot (q_{j/1} L_{46})^{3/2}}{\gamma_{j,5}^{7/4} \cdot u_3^{3/4}}. \quad (6)$$

This result is based on the investigation of a quasar sample, described in detail in [Falcke and Biermann (1995)]. The disk luminosity is connected to the integral radio luminosity, L^s , as

$$L_{\text{disk}} = (21.6 \pm 16.6) \cdot 10^{45} \cdot (1+z)^{-1/2} (L_{42}^s)^{2/3}, \quad (7)$$

assuming a spectral index of $\alpha = 0.8$. Again, the error has been estimated considering the scattering of the data by a factor three around the predicted result. The parameters which occur in Equ. (4) and (6) are given below.

PARAMETER LIST

- β_j : Jet velocity in units of c which can be assumed to have a value of $\beta_j \approx 0.986$.
- γ_j : jet's Lorentz Boost factor, $\gamma_j = 6$.
- P_{-12} : Pressure parameter. The external radiation pressure at the AGN is given by $P_{ext} = P_{-12} \cdot 10^{-12} \text{ erg/cm}^3$. The pressure evolves with the time due to the expansion of the Universe. The pressure parameter depends on the redshift as $P_{-12} = (1+z)^3 \cdot P_{-12}^0$, where P_{-12}^0 is the pressure of the Universe at $z = 0$. P_{-12}^0 is set to $P_{-12}^0 = 1$.
- $x'_{e,100}$: Modified electron density. Let the ratio between the relativistic electron density and the total number density of protons be x_e and the minimum Lorentz factor of the relativistic electron population divided by 100, $\gamma_{e,100}$. The modified electron density is then $x'_{e,100} = \gamma_{e,100}^{p-1} x_e$. $p = 2$ is a parameter. $x'_{e,100} \approx 1$ has been used in all following calculations [Falcke and Biermann (1995)].
- $q_{j/1}$: Total jet power Q_{jet} in units of the disk luminosity, with a given value of $q_{j/1} = Q_{jet}/L_{disk} = 0.15_{-0.1}^{+0.2}$.
- L_{46} : Disk luminosity per 10^{46} erg/s : $L_{46} = L_{disk}/(10^{46} \text{ erg/s})$.
- $\gamma_{j,5}$: Jet's Lorentz boost factor, divided by 5. It is assumed to be $\gamma_{j,5} = (6 \pm 2)/5$.
- u_3 : Ratio between the total energy density in the jet and the magnetic energy density, divided by a factor three. It is set to $u_3 = 1$ [Falcke et al. (1995)]. Note, again, that this fits the observations best.
- $\xi = 0.15$: Fit parameter resulting from the ansatz that the bulk proper velocity depends on the accretion rate and thus on the disk luminosity, see [Falcke and Biermann (1995)].
- $i_{obs} = 1/\gamma_j = 1/6$: angle between observer and jet axis. The angle is taken to be $1/\gamma_j$, because this is the maximal boosting range and has a solid angle in which optimal boosting occurs. We use for simplicity the same angle for all sources: In a more refined model obviously isotropy should be used, but then mediated by the selection effects, which strongly favor small angles, as are used here.
- $D = \frac{1}{\gamma_j} (1 - \beta_j \cos i_{obs})^{-1} \approx 6$: Doppler factor. In this calculation, the Doppler factor is assumed to be the same for all sources. A variation of the Doppler factor with the source luminosity has been discussed - for an example see e.g. [Falcke et al. (1995)]. However, since there is no well-founded model to apply individual Doppler factors so that a constant factor has to be used as an approximation.

Finally, the jet-disk symbiosis can be used to express the generic neutrino energy spectrum in terms of the radio luminosity in units of 10^{42} erg/s . The result at a luminosity of $L_{42} = 100$ with varying spectral index is shown for steep spectrum sources in Fig. 4 and in Fig. 5 for flat spectrum sources. The power law decrease can be observed up to a cut energy at $E_\nu \sim 10^9 \text{ GeV}$,

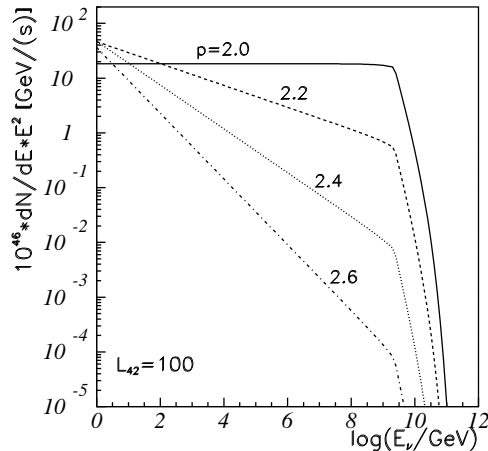


Fig. 4. Energy dependence of the generic AGN neutrino spectrum of steep spectrum sources. The normalization is dependent on the particle index p , shown for $p = 2.0, 2.2, 2.4, 2.6$. The radio luminosity is assumed to be $L_{42} = 100$.

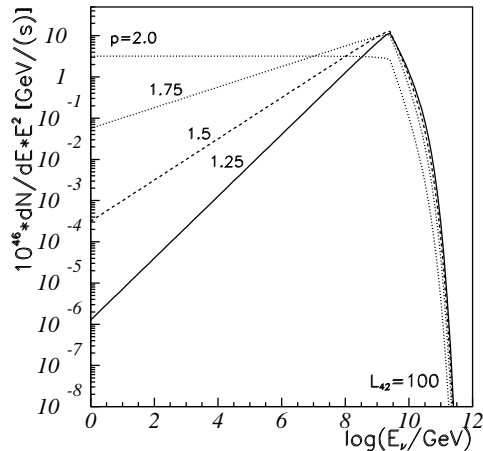


Fig. 5. Energy dependence of the generic AGN neutrino spectrum flat spectrum sources. The spectrum is shown at $L_{42} = 100$ and for three different particle indices, $p = 1.25, 1.50, 1.75, 2.0$.

where synchrotron losses of the neutrino-producing pion start to show as well as the exponential cutoff of the spectrum.

4 Integration limits

The integration over the luminosity has to be performed before the redshift integration, since the lower luminosity limit implicitly depends on the redshift. The limits for the z -integration are taken to be

$$z_{\min} = 0.03$$

$$z_{\max} = 6.$$

The minimum of the z -integration is given by the fact that the flux is assumed to be diffuse. For $z < 0.03$, a contribution from the supergalactic plane is expected as will be discussed in section 5. The maximum redshift is taken to be $z = 6$, since the total z dependence decreases rapidly with redshift and any contribution above z_{\max} can be neglected as can be seen in Fig. 6 (steep spectrum sources) and Fig. 7 (flat spectrum sources). Up to $z = 6$, the consistency of the used models is ensured, since AGN have been detected up to redshifts of $z \approx 6.4$ [Willott et al. (2003)].

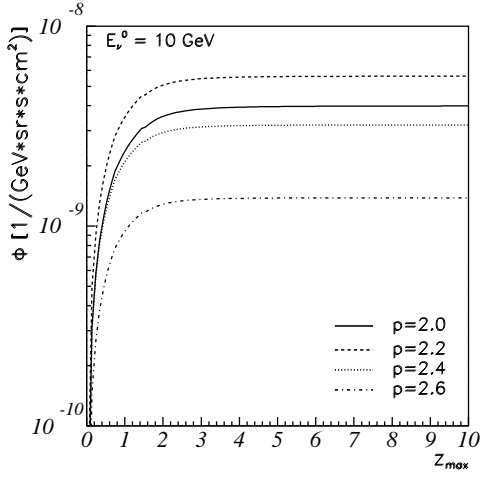


Fig. 6. Neutrino flux with variation of the upper redshift integration limit z_{\max} for steep spectrum sources. The neutrino energy is set to $E_\nu^0 = 10$ GeV while the particle index is varied as $p = 2.0, 2.2, 2.4, 2.6$.

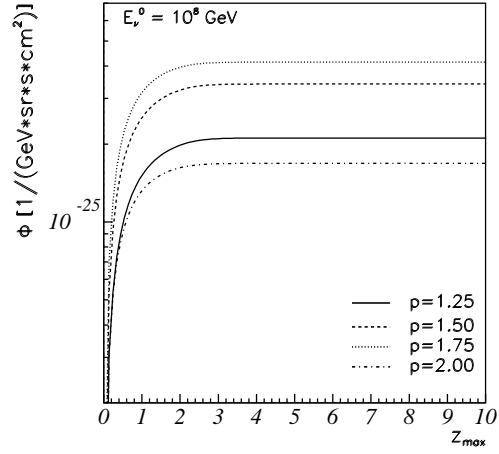


Fig. 7. Neutrino flux with variation of the upper redshift integration limit z_{\max} for flat spectrum sources. The neutrino energy is set to $E_\nu^0 = 10^8$ GeV while the particle index is varied as $p = 1.25, 1.50, 1.75, 2.00$.

The maximum radio luminosity limit is taken to be $L_{42}^{\max} = 10^4$. Fig. 8 (steep spectrum sources) and 9 (flat spectrum sources) show the dependence of the flux at $z = 2$ and $E_\nu^0 = 10^8$ GeV (flat) respectively $E_\nu^0 = 10$ GeV. The contribution is negligible for $L_{42} > 10^3$ in the case of steep spectrum sources and for $L_{42} > 10$ in the case of flat spectrum sources. This shows that most of the contribution to the flat spectrum neutrino flux comes from sources with moderate luminosities, $L_{42} < 10$. The highest contribution to the flat spectrum neutrino flux comes from sources with luminosities around $L_{42} \approx 300 - 1000$.

The lower radio luminosity limit depends on the following facts:

- (1) The absolute lower limit: For the model of *extended sources*, the jet-disk symbiosis is developed for FR-II galaxies and the absolute lower limit, $L_{42,\min}^s$, is given by the lower luminosity limit for FR-II galaxies which is given as $L_{0.178} \approx 2.5 \cdot 10^{26}$ W/Hz with an integral radio luminosity of approximately $L_{42,\min}^s = 10$. The sample of *flat spectrum sources*, on the other hand, ranges from $10^{-1.5} < L_{42}^f < 10^4$ and the absolute lower limit, $L_{42,\min}^f$ is thus $L_{42,\min}^f = 10^{-1.5}$.
- (2) The maximum proton energy which can be produced by an AGN is connected with the disk luminosity according to Lovelace (1976):

$$E_p^{\max} = C' \cdot \sqrt{L_{46}} \quad (8)$$

up to a luminosity of $L_{46} \approx 1$, where the relation saturates,

$$E_p^{\max} = C' . \quad (9)$$

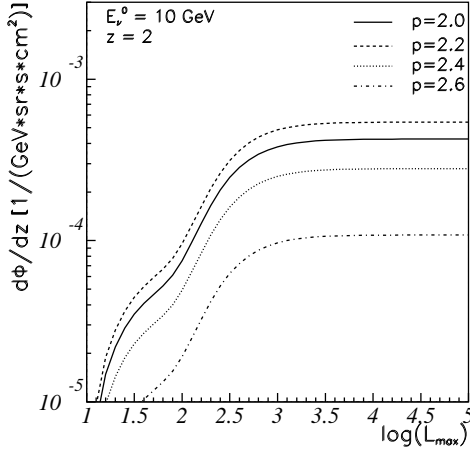


Fig. 8. Variation of the steep spectrum source neutrino flux with the upper integration limit, using different spectral indices, $p = 2.0, 2.2, 2.4$ and 2.6 . The redshift is arbitrarily taken to be $z = 2$, the energy is set to $E_\nu^0 = 10$ GeV. The flux normalization is saturated at approximately $L_{\max} \approx 10^3$.

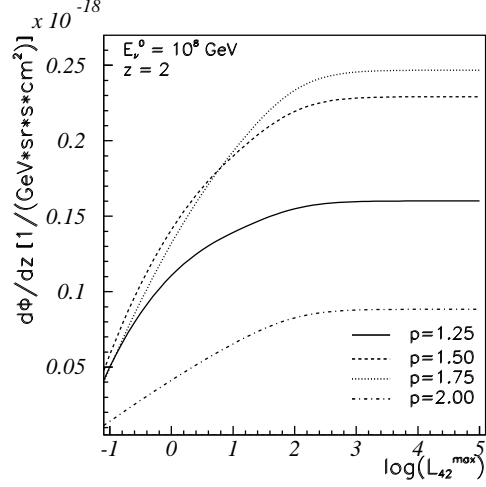


Fig. 9. Variation of the neutrino flux (flat spectrum sources), using $p = 1.25, 1.5, 1.75$ and 2.00 . The redshift is chosen to be $z = 2$ and the energy is set to $E_\nu^0 = 10$ GeV. Sources at $L > 10$ do not contribute significantly to the flux.

The result is supported by the jet-disk symbiosis model, see [Falcke and Biermann (1995)]. Taking the highest observed energy so far, $E_p \approx 10^{21}$ eV and the maximum luminosity, $L_{disk}^{\max} = 10^{47}$ erg/s, the constant C' is determined to be $C' = 10^{11.5}$ GeV. When the jet-disk symbiosis model by Falcke et al. is used and the ratio between E_p and E_ν taken to be $20/1$, the maximum neutrino energy is correlated to the radio luminosity due to the non linear relation between radio and disk luminosity,

$$E_\nu^{\max} = C \cdot L_{42}^\beta.$$

This numerical relation is consistent with inserting all known parameters for the radio galaxy M87. C and β are given by the corresponding relations between disk and radio luminosity for flat or steep spectrum sources and are listed in table 3.

Therefore, the lower luminosity limit of an AGN contributing to a certain flux at a fixed neutrino energy is

$$L_{42}^{\min} = \max\left\{L_{42,\min}^{s/f}, \left(\frac{E_\nu}{C}\right)^{1/\beta}\right\}. \quad (10)$$

The contribution to the flux for an energy corresponding to a luminosity exceeding $L_{disk} = 10^{46}$ erg/s, that is energies of $E_\nu = C'/20 =$

	C [GeV]	β	E_ν^{cut} [GeV]
steep	$2.2 \cdot 10^{10} \cdot (1+z)^{-1/4}$	1/3	$\sim 5 \cdot 10^9 (z=2)$
flat	$7.5 \cdot 10^9$	0.3935	$\sim 2 \cdot 10^8$

Table 3

Parameters for the determination of the lower luminosity integration limit.

$10^{11.5}$ GeV $\approx 2 \cdot 10^{10}$ GeV is insignificantly small.

Since the RLF is decreasing with luminosity, the energy spectrum will steepen from that energy on, when the luminosity-energy relation exceeds the value of the absolute luminosity limit, $\left(\frac{E_\nu}{C}\right)^{1/\beta} \geq L_{42,\min}^{f/s}$. This is the case for an energy

$$E_\nu^{cut}/\text{GeV} \approx (L_{42,\min}^{s/f})^\beta \cdot C/\text{GeV} \quad (11)$$

in the comoving frame. The cut energies for the two models are given in table 3.

5 Results

5.1 Discussion of the spectra varying the particle index

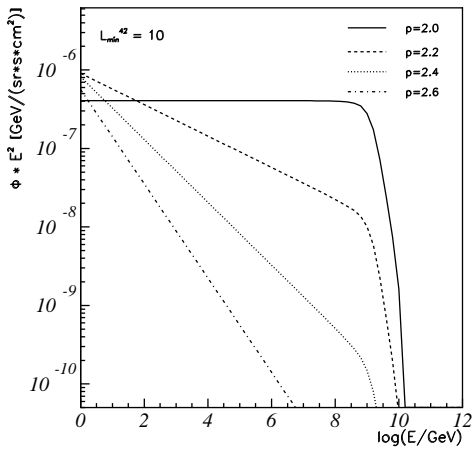


Fig. 10. Neutrino spectrum of steep spectrum AGN. The particle index is varied ($p = 2.0, 2.2, 2.4, 2.6$).

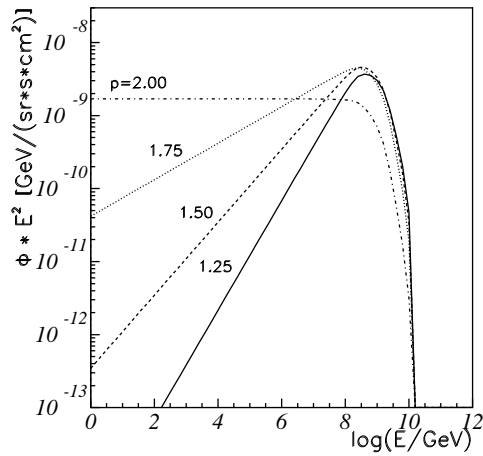


Fig. 11. Neutrino spectrum of flat spectrum AGN for different particle indices $p = 1.25, 1.50, 1.75, 2.00$.

The final steep spectrum source flux is shown in Fig. 10. The spectrum is presented for four different particle indices, $p = 2.0, 2.2, 2.4, 2.6$. Here, $p = 2$ is a commonly used value in literature and $p = 2.6$ has been computed in section 2 from the spectral index at $2.7 - 5$ GHz for the steep spectrum population. The spectrum decreases as a power law up to a cut energy at approximately 10^9 GeV. At higher energies, the spectrum is falling more rapidly due to pion synchrotron loss effects and the exponential cutoff of the spectrum. For a particle index of $p = 2$, the flux is approximately

$$E^2 \Phi^s \approx 10^{-7} \text{GeV}/(\text{s sr cm}^2)$$

for one neutrino flavor. This is very close to the current neutrino flux limit derived from the observed atmospheric muon and anti muon neutrino spectrum

$$E^2 \Phi < 2.6 \cdot 10^{-7} \text{GeV}/(\text{s sr cm}^2)$$

at energies around 300 TeV [Woschnagg and AMANDA Collaboration (2004)]. The flat source neutrino spectrum is shown in Fig. 11 with a spectral index of $p = 1.25, 1.50, 1.75$ and 2.00 . The cut energy lies at $E \sim 10^9$ GeV as discussed before. Values $p \neq 2$ are shown as a comparison, the final result will be given for $p = 2$ as indicated by diffuse shock acceleration. For $p = 2$, the flux is

$$E^2 \Phi^f \approx 10^{-9.2} \text{GeV}/(\text{s sr cm}^2)$$

for one neutrino flavor. This is about two orders of magnitude lower than the prediction for steep spectrum sources.

5.2 Discussion of Uncertainties

Apart from the lack of knowledge of the exact optical depth, the calculation of the neutrino flux Φ bears uncertainties $\Delta\Phi$ because of two reasons: It is still a challenging task to make a precise prediction of the objects' redshift. Thus, the RLFs include high uncertainties for very distant objects. Nevertheless, the functions are quite well known up to a redshift of $z \approx 2$. Since objects at a higher redshift do not contribute significantly to the diffuse neutrino spectrum, the error due to uncertainties in distance measurements will be neglected compared to uncertainties in the jet-disk symbiosis model.

The jet-disk symbiosis model agrees with the data when allowing a scattering of a factor of three in a $L_{radio}(L_{disk})$ graph. This transfers to an uncertainty of $\Delta\phi_\nu = 0.78 \cdot \phi_\nu$, that means the an uncertainty of a factor ~ 2 towards higher and a factor ~ 5 towards lower fluxes. The spectrum for flat spectrum sources

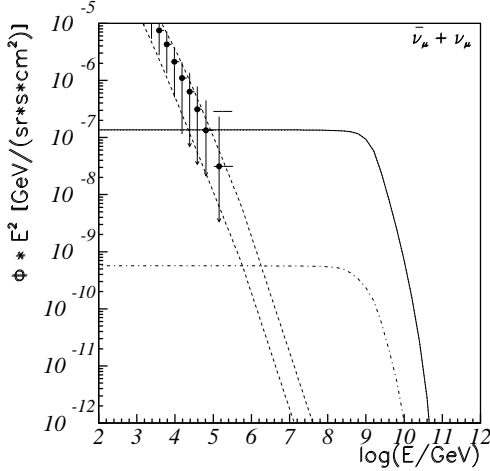


Fig. 12. AGN $\nu_\mu + \bar{\nu}_\mu$ neutrino spectrum with an index of $p = 2$. The flat spectrum sources (dotted line) do not contribute significantly compared to the steep spectrum population - the solid line represents the sum of flat and steep spectrum sources which does not differ from the result for steep spectrum sources. The data points result from unfolding the AMANDA neutrino spectrum. They follow the conventional atmospheric neutrino spectrum (dashed lines) and an upper limit is derived as is indicated in the figure [Woschnagg and AMANDA Collaboration (2004)].

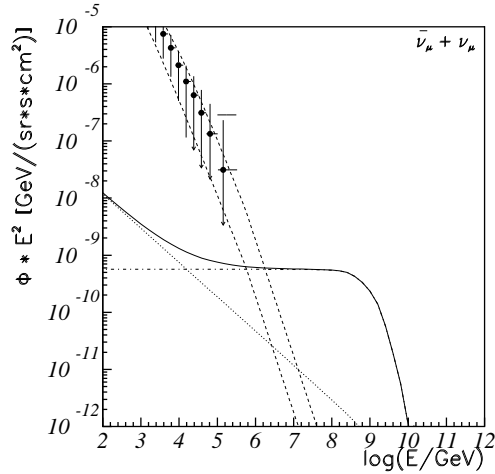


Fig. 13. AGN $\nu_\mu + \bar{\nu}_\mu$ neutrino spectrum with an index of $p = 2.6$ for steep spectrum sources and $p = 2.0$ for flat spectrum sources. The steep spectrum sources (dot-dashed line) make up most of the spectrum at lower energies ($E_\nu > 10^6$ GeV). The flat spectrum sources (dotted line) dominate the total spectrum (solid line) at energies of $E_\nu > 10^6$ GeV. A signal that exceeds the atmospheric contribution is expected starting at $E_\nu \approx 10^8$ GeV.

includes an uncertainty of $\Delta\phi_\nu^f = 0.9 \cdot \phi_\nu$ which means a factor of ~ 2 above an a factor of 10 below the prediction.

Uncertainties due to the chosen cosmology would result in another factor of two in the change of the normalization.

Since the maximum energy of the spectrum depends on the disk luminosity which is converted into a radio luminosity using the jet-disk symbiosis model, the cutoff may change by an order of magnitude at most.

5.3 Discussion of a source flux from the supergalactic plane

It has been stated before that the calculations include sources at $z > 0.03$ to exclude possible anisotropies from the supergalactic plane. In the following paragraph, a possible flux from the supergalactic plane will be discussed. Note that this is just to make an estimate of a possible contribution from nearby

sources and that final results do not include sources at $z < 0.03$. Assuming that the contribution to the total flux at $z < 0.03$ is concentrated in the supergalactic plane yields an increase of the flux by a factor 10 since the supergalactic plane, [Lahav et al. (2000)], covers approximately 10 % of the sky. The ratio of the diffuse steep spectrum flux at $z > 0.03$ and the flux from the supergalactic plane is of the order

$$\frac{\Phi^{steep}(z < 0.03)}{\Phi^{steep}(z > 0.03)} \approx 0.01 .$$

Since this is only some percent of the total diffuse flux, it is negligible. For flat spectrum sources, the result is

$$\frac{\Phi^{flat}(z < 0.03)}{\Phi^{flat}(z > 0.03)} \approx 0.02$$

and thus also negligible compared to the flux from outside the supergalactic plane.

5.4 Discussion of the final spectra

The comparison of the two source type spectra considering only one neutrino flavor¹ in Fig. 12 shows that the dominant contribution comes from steep spectrum sources assuming a particle index of $p = 2.0$. However, using $p = 2.6$ for the steep source spectrum reduces the contribution from this sample significantly as is presented in Fig. 13. The cutoff in the energy spectrum at $E_\nu \sim 10^9$ GeV occurs since the maximum energy for each single source depends on the source luminosity as shown by Lovelace (1976) and Falcke and Biermann (1995). Thus, the cutoff energy of the isotropic distribution depends on the sources' luminosity distribution. The atmospheric neutrino spectrum (dashed lines) dominates the spectrum up to energies of $\sim 10^7$ GeV.

The maximum optical depth of the sources can be estimated by assuming that the contribution of the calculated spectrum has to be smaller than the limit set by AMANDA mentioned above. Thus, in case of an E^{-2} spectrum for steep spectrum sources, the optical depth can be restricted to $\tau_{eff} < 2$. This factor will grow significantly when using an $E^{-2.6}$ spectrum, i.e. $\tau_{eff} < 1000$. For flat spectrum sources, an effective opacity of $\tau_{eff} < 400$ can be estimated.

¹ The total flux is divided by a factor of three, taking into account neutrino oscillations.

A comparison of the results using two different spectral indices for the steep spectrum sources makes clear how much the total flux contribution depends on the spectral index of the sources. Changing the spectral index from $p = 2.0$ to $p = 2.6$ reduces the contribution from the source sample by two orders of magnitude. In the pessimistic case, the detection of a signal from these types of AGN will require an array like IceCube or Auger which are sensitive to UHE neutrinos at $\sim 10^{19}$ eV. In the case of an E^{-2} spectrum the detection of a diffuse signal should be possible in the near future. Fig. 14 shows a summary of various extragalactic neutrino flux predictions, see [Learned and Mannheim (2000)] for a review. In the usual E^{-2} scenario, the AGN spectrum should be detectable in the very near future, presumably already by running neutrino experiments like AMANDA. If the spectrum is steeper, however, it has been shown that a detection of a significant neutrino signal from AGN would need some years of operation of a km^3 experiment like IceCube.

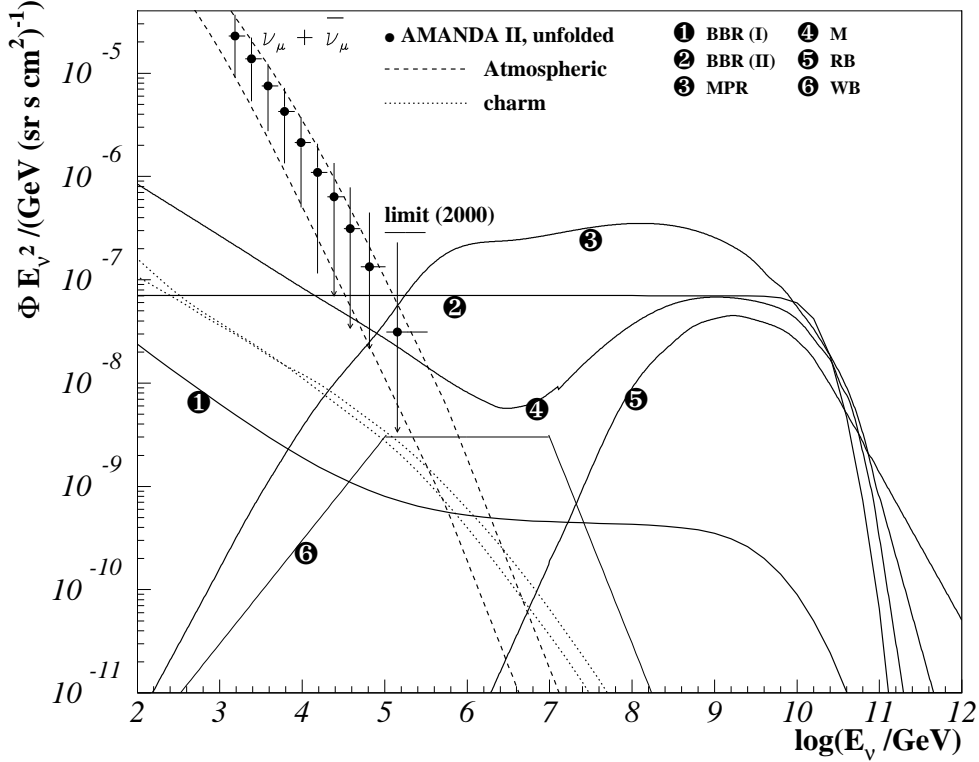


Fig. 14. $\nu_\mu + \bar{\nu}_\mu$ neutrino flux predictions. (1) and (2) are the predictions done in this paper, BBR(I) using $p = 2.6$ for the steep spectrum sources, BBR(II) applying $p = 2$; (3): $p\gamma$ interactions, MPR [Mannheim et al. (2001)]; (4): M [Mannheim (1995)], $p\gamma$ in blazar and pp in its host galaxy; (5): RB [Rachen and Biermann (1993)], $p\gamma$; (6): WB [Waxman and Bahcall (1999)], diffuse neutrino flux from GRBs, assuming that GRBs are the sources of cosmic rays at $E > 10^{19}$ eV. The dashed lines indicate the atmospheric neutrino spectrum according to Volkova and Zatsepin (1980), the upper line representing the horizontal flux, the lower line showing the vertical contribution. The dotted lines represent a model for the atmospheric charm contribution as predicted in [Martin et al. (2003)]. The uncertainties in the model occur due to larger errors in measurements of the Björken variable in forward scattering. Data points are AMANDA data showing the unfolded spectrum of 2000 data. It follows the atmospheric prediction. The limit on the extraterrestrial neutrino flux is set based on the data from the last bin of the unfolded spectrum [Woschnagg and AMANDA Collaboration (2004)].

6 Acknowledgments

The authors would like to thank K. Mannheim and H. Falcke for valuable discussions which led to much progress in realizing this work.

The work with P. L. Biermann has been supported through the AUGER theory and membership grant 05 CU1ERA/3 via DESY/BMBF (Germany). Further support for the work with P. L. Biermann has come from the DFG, DAAD, Humboldt Foundation (all Germany), grant 2000/06695-0 from FAPESP (Brasil) with G. Medina-Tanco, a grant from KOSEF (Korea) through H. Kang and D. Ryu, a grant from ARC (Australia) through R. J. Protheroe, and a European INTAS grant with V. Berezhinsky. Special support comes from the European Sokrates/Erasmus grants in collaboration with East-European Universities, with partners M. Ostrowski, K. Petrovay, L. Gergely, A. Petrusel, and M.V. Rusu, and VIHROS through the FZ Karlsruhe. Current support comes from NATO for a collaboration with S. Moiseenko and G. Bisnovaty-Kogan (Moscow), and the Chinese Academy of Sciences of China in work with Y. Wang (Beijing/Nanjing).

References

- Biermann, P. L., 2001. High energy particles in Active Galactic Nuclei. In: Shapiro, M. M., et al. (Eds.), Kluwer Acad. Publ. p. 115, review at the Erice school Nov. 2000.
- Biermann, P. L., Strittmatter, P. A., 1987. *apj* 322, 643.
- Bridle, A. H., Perley, R. A., 1984. *Ann. Rev. Astron. Astrophys.* 22, 319.
- Dunlop, J. S., Peacock, J. A., 1990. *Month. Not. Roy. Astr. Soc.* 247, 19.
- Falcke, H., Biermann, P. L., 1995. *Astron. & Astrophys.* 293, 665.
- Falcke, H., Malkan, M. A., Biermann, P. L., 1995. *Astron. & Astrophys.* 298, 375.
- Gregorini, L., et al., 1984. *Astron. J.* 89, 323.
- Hillas, A. M., 1984. The Origin of Ultra-High-Energy Cosmic Rays. *Ann. Rev. Astron. Astrophys.* 22, 425.
- IceCube Collaboration, 2004. *Astropart. Physics* 20, 507.
- Kühr, H., et al., 1981. *Astron. J.* 86, 854.
- Lacy, M., et al., 1999. *Month. Not. Roy. Astr. Soc.* 308, 1096.
- Lahav, O., et al., 2000. *Month. Not. Roy. Astr. Soc.* 312, 166.
- Laing, R. A., Riley, J. M., Longair, M. S., 1983. *Month. Not. Roy. Astr. Soc.* 204, 151.
- Learned, J. G., Mannheim, K., 2000. *Annu. Rev. Nucl. Part. Sci.* 50, 679.
- Lovelace, R. V., 1976. *Nature* 262, 649.
- Mannheim, K., 1995. *Astropart. Physics* 3, 295.
- Mannheim, K., Protheroe, R. J., Rachen, J. P., 2001. *Phys. Rev. D* 63, 23003.
- Martin, A. D., Ryskin, M., Stasto, A., 2003. *Acta Phys. Polon.* B34, 3273.
- McGilchrist, M. M., Riley, J. M., 1990. *Month. Not. Roy. Astr. Soc.* 246, 123.
- Miyaji, T., Hasinger, G., Schmidt, M., 2000. *Astron. & Astrophys.* 353, 25.
- Montaruli, T., 2003. In: *Particle Astrophysics Instrumentation*. Edited by Peter W. Gorham. Proceedings of the SPIE, Volume 4858. p. 92.
- Mücke, A., et al., 1999. *Publ. Astron. Soc. Aust.* 16, 160.
- Mücke, A., et al., 2000. *Comput. Phys. Commun.* 124, 290.
- Particle Data Group, 2004. *Phys. Let. B* 592, 1, Particle Physics Booklet.
URL <http://pdg.lbl.gov>
- Pauliny-Toth, I. I. K., Kellermann, K. I., 1972. *Astron. J.* 77, 797.
- Pauliny-Toth, I. I. K., et al., 1972. *Astron. J.* 77, 265.
- Pauliny-Toth, I. I. K., et al., 1978. *Astron. J.* 83, 451.
- Peacock, J. A., 1985. *Month. Not. Roy. Astr. Soc.* 217, 601.
- Peacock, J. A., Wall, J. V., 1981. *Month. Not. Roy. Astr. Soc.* 194, 331.
- Protheroe, R. J., 1998. In: *Towards the Millennium in Astrophysics, Problems and Prospects*. International School of Cosmic Ray Astrophysics 10th Course. p. 3.
- Rachen, J. P., Biermann, P. L., 1993. *Astron. & Astrophys.* 272, 161.
- Rawlings, S., Eales, S., Lacy, M., 2001. *Month. Not. Roy. Astr. Soc.* 322, 523.
- Rybicki, G. B., Lightman, A. P., 1979. *Radiative processes in astrophysics*. J. Wiley & Sons, Inc.
- Schechter, P., 1976. *Astrophys. J.* 203, 297.
- Spergel, D. N., et al., 2003. *Astrophys. J. Sup. S.* 148, 175.
- Volkova, L. V., Zatsepin, G. T., 1980. *Sov. J. of Nuc. Phys.* 37, 212.
- Wall, J. V., Peacock, J. A., 1985. *Month. Not. Roy. Astr. Soc.* 216, 173.

- Waxman, E., Bahcall, J., 1999. *Phys. Rev. D* 59, 23002.
- Willott, C. J., McLure, R. J., Jarvis, M. J., 2003. *Astrophys. J. Let.* 587, L15.
- Willott, C. J., et al., 2001. *Month. Not. Roy. Astr. Soc.* 322, 536.
- Woschnagg, K., AMANDA Collaboration, 2004. *Astro-ph/0409423*, talk at Neutrino 2004.
- Wright, A. E., et al., 1982. *Austr. J. of Phys.* 35, 177.